

# Consideration on Response of Seismic Isolated Elevated Bridges due to Slightly Strong Earthquakes

Xiang YIN<sup>1</sup> · Yoshikazu TAKAHASHI<sup>2</sup>

<sup>1</sup> Student, Department of Civil and Earth Resources Engineering, Kyoto University, Kyoto, Japan  
yin.xiang.48a@st.kyoto-u.ac.jp

<sup>2</sup> Professor, Department of Civil and Earth Resources Engineering, Kyoto University, Kyoto, Japan  
takahashi.yoshikazu.4v@kyoto-u.ac.jp

**ABSTRACT:** In this study, in order to grasp the special quality of seismic isolators and clarify the behavior of seismic isolated structure at actual slightly strong earthquake (M 4.0 ~ M6.9), system identification has been used to analyze the behavior of seismic isolated structures under slightly strong earthquakes with the response record of a seismic isolated structure under main shock of the earthquake in Osaka-Fu Hokubu on 18th June 2018. The objective structure, Pier 408 of Matsunohama Viaduct is located in the southwest direction, 30 km away from the epicenter.

**Keywords:** Seismic Isolation; Elevated Bridge; 2018 Osaka-Fu Hokubu Earthquake

## 1. INTRODUCTION

Japan is one of the countries located in earthquake prone regions and structures often become the victims of earthquakes. Many cases of structures collapse occurred when being exposed to past strong earthquakes. Owing to the collapse of structures, society suffered enormous costs and inconveniences. Meanwhile, elevated bridges are one of the most important parts in nowadays transportation networks, which are considered as the lifeline structures. Since they play an essential role in domestic transportation supporting the daily functions and needs, they also required higher seismic performance than standard structures. Aim to improve the seismic performance of structures during earthquakes, the number of the structures using seismic base isolated devices has an increasing tendency after past large-scale earthquakes like the Great Hanshin Earthquake (1995 Kobe Earthquake) and Great East Japan Earthquake (2011 Tohoku Earthquake). The number of earthquakes occurring in Japan in the average of one year is shown in **Fig.1** and the calculation was based on the data collected from 2001 to 2011 by Japan Meteorological Agency. From this figure, we can see that the large-scale earthquake (>M 7.0) rarely occurs, however, the slightly strong earthquakes (M 4.0 ~ M6.9) frequently occurs. Several researches have been carried out on analyzing the behavior of seismic base isolated structures during large scale earthquakes however, few researches have been done on analyzing the response of seismic base isolated structure due to slightly strong earthquakes. The deformation and shear strain of the seismic base isolated devices in slightly strong earthquakes are much smaller compared to that in large scale earthquakes. Therefore, analyzing the characteristics of the seismic base isolated bearings such as stiffness and damping ratio in small shear strain region are extremely necessary and the accuracy of restoring force model for seismic base isolated devices is also one of the most important issues that need

to be taken into consideration. In this study, system identification was performed by using the response record of the seismic base isolated structure observed in the main shock during the earthquake in Osaka-Fu Hokubu on 18 June 2018. The earthquake is measured as Magnitude 6.1 with its epicenter (Latitude 36.1N, Longitude 139.9E) in the Takatsuki area of northeastern Osaka, at a depth of 13.2 kilometers. Shaking from the earthquake was felt strongly in the prefecture and the nearby areas such as Hyogo Prefecture and Kyoto Prefecture and it also had varying degrees of damage or effect to the structures around the epicenter. The objective structure, Pier 408 of the Matsunohama Viaduct is located 30 km west-southeast away from the epicenter of the earthquake as shown in **Fig.2**.

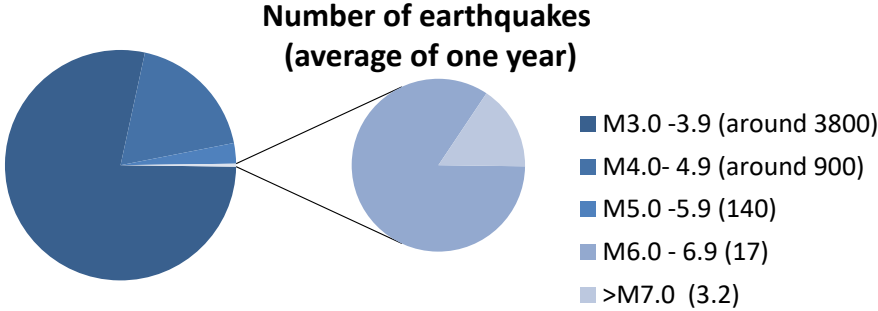


**Fig.1** Number of earthquakes occurring in Japan in the average of one year

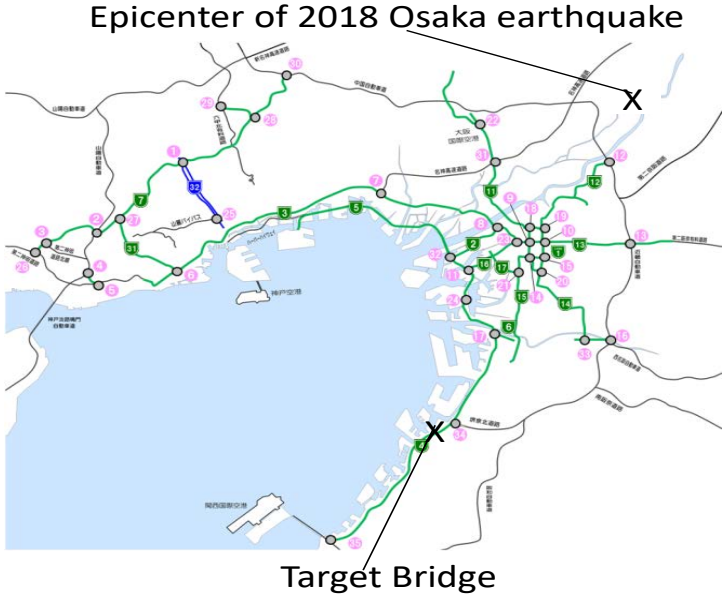
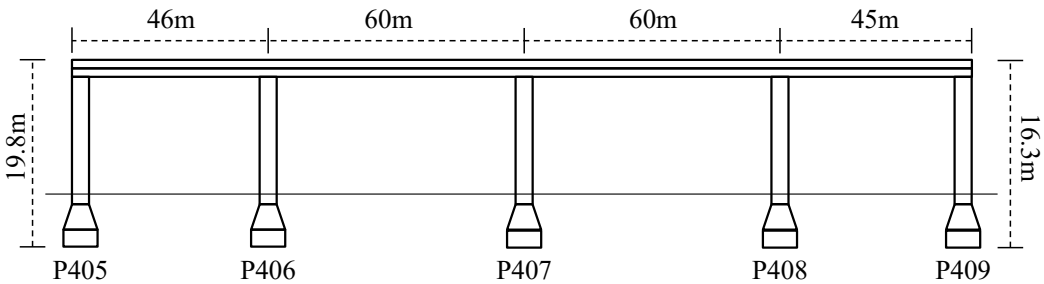


**Fig.2** The location of the target structure

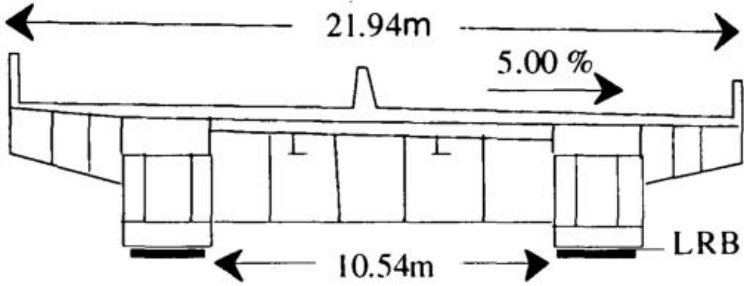
**2. DESCRIPTION OF THE TARGET BRIDGE**

The objective bridge, Matsunohama Viaduct is situated on the Bay Shore route of Hanshin No. 5 Expressway in Izumiotsu Prefecture, which is located at 30 km west-southeast away from the epicenter of the earthquake in Osaka-Fu Hokubu on 18 June 2018 and the seismic acceleration response has been recorded during the earthquake. Matsunohama Viaduct is one of the pioneer structures with special consideration for earthquake resistant design and lead rubber bearings (LRBs) are used to improve the seismic response of the viaduct. The target bridge was built in 1991 and a seismic reinforcing work was been done in November 1995, 10 months after the Kobe earthquake. As shown in **Fig.3**, this four-span-

continuous bridge has an overall length of 211.5 m. The two middle spans are 60 m, and the side spans are 46.5 and 45 m. The superstructure consists of two non-composite steel box girders and is supported by lead rubber bearings (LRBs) at the inner piers (P406 to P408) and on pivot roller bearings at the end piers (P405 and P409). Bearings can move only in the longitudinal direction and two side stoppers installed with 5-mm clearance prevent movement in the transverse direction. Reinforced concrete, single-column T shaped piers, founded in pile caps, are used for the substructure, and groups of the cast in place reinforced concrete piles of 1.2 m diameter are used for the foundation. The plan view and side view of the LRBs are shown in Fig.4 .According to the expereriment data from Hanshin Expressway, the loading test results when the shear strain is 4% and 70% are shown in Fig.5.[1] From the force-displacement relationship graph, we can pick up that the corresponding equivalent stiffness are  $75460N/mm$ ,  $49000N/mm$  and  $14210N/mm$  when the shear strain is 1.5%, 4% and 70% respectively. In this study, since the shear strain 1.5% is small enough, we define the corresponding stiffness as the experimental primary stiffness. According to the Design Specification for highway bridges bearings, its primary stiffness is smaller than experimental primary stiffness since it represents the stiffness when the shear strain is around 80%. Additionally, Pier P408 is instrumented with four seismometers for research at one meter underground, footing, pier top and girder. When the earthquake occurs, seismometers are able to record acceleration in the vertical, transverse and longitudinal direction of the bridges axis at a data-sampling rate of 100 KZ.



(a)Longitudinal Elevation of the bridge



(b)Cross Section of the superstructure

Fig. 3 Elevation and Cross Section

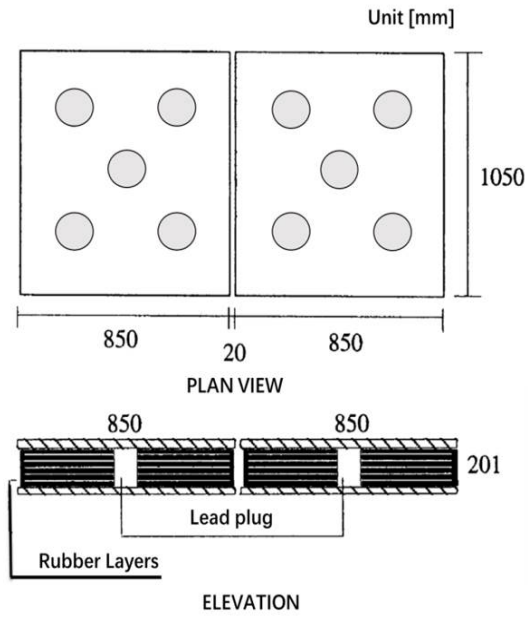
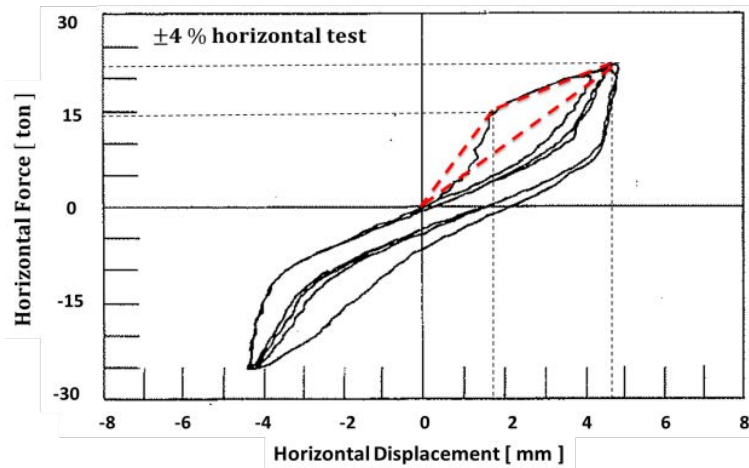
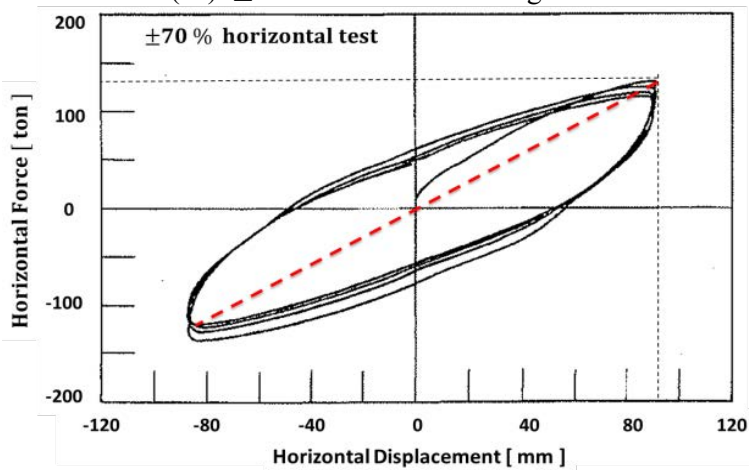


**Fig. 4** The plan view and side view of LRBs



( a ) ±4% Horizontal Loading Test



( b ) ±70% Horizontal Loading Test

**Fig.5** Loading test result

### 3. OBSERVATION RECORDS

The acceleration record observed in the main shock during the earthquake in Osaka-Fu Hokubu on 18 June 2018 is shown in **Fig.6** and the maximum response acceleration is summarized in **Table1**. From the acceleration response spectrum in longitudinal direction shown in **Fig.7**, we can easily find out that the peak of footing appears at around 0.38 seconds, the peak of pier top appears at around 0.18 seconds and the peak of girder appears at around 0.12 seconds.

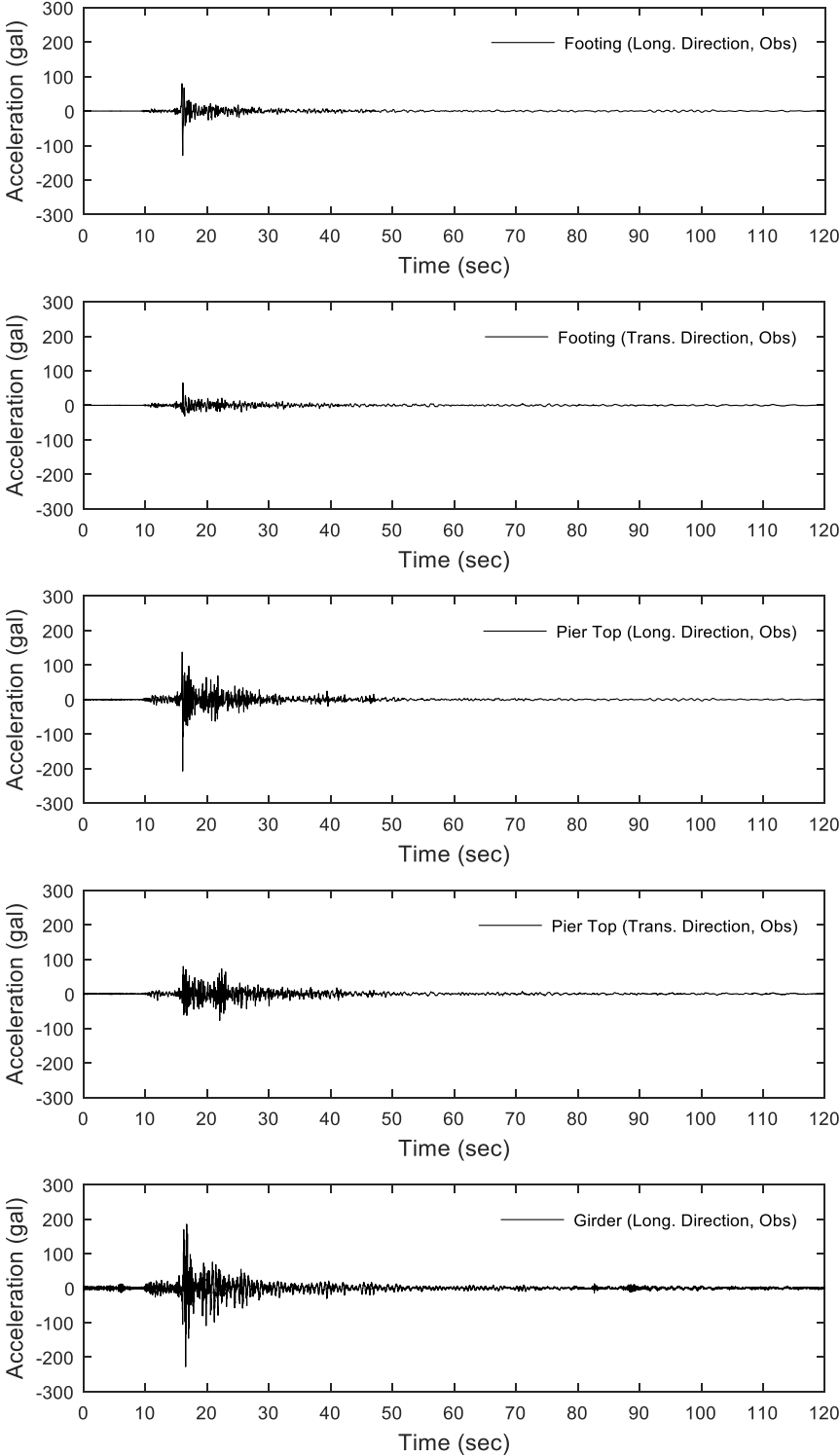


**Fig.6** The acceleration observation record

**Table1** Maximum response acceleration

	MAX [gal]
Footing (Long.)	128.65
Pier Top (Long.)	207.22
Girder (Long.)	227.76
Footing (Trans.)	65.15
Pier Top (Trans.)	79.65

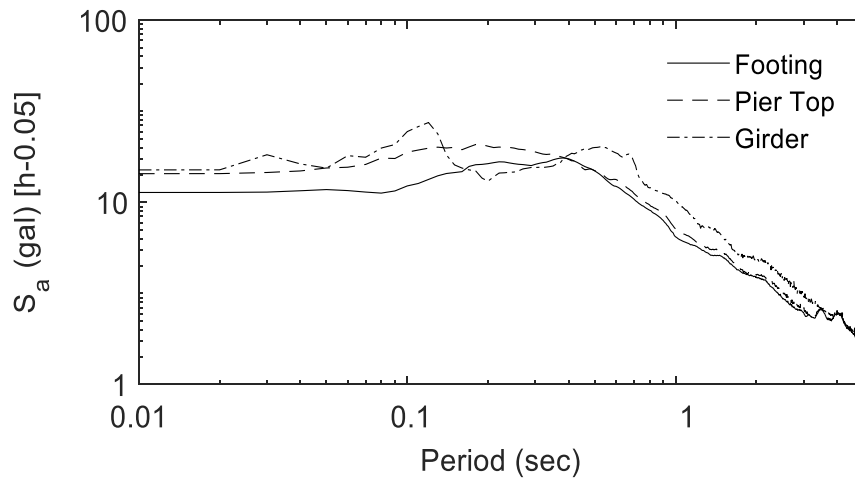


**Fig.7** Acceleration response spectrum in Long. Direction

### 3. METHODOLOGY AND MODELLING

**Fig.8** shows the outline of the identification method. When earthquake happens, the acceleration and the velocity of the ground motion will be recorded. At the same time, the superstructure will also have a acceleration and velocity response. In the next step, the structure will be modelled multi-degree of freedom system. By inputting the acceleration and velocity of the ground motion and setting the parameters such as stiffness and the damping ratio, we can get the acceleration and velocity response of the model. After comparison between the observation and the output, we will change the parameter manually to find a best fit output.

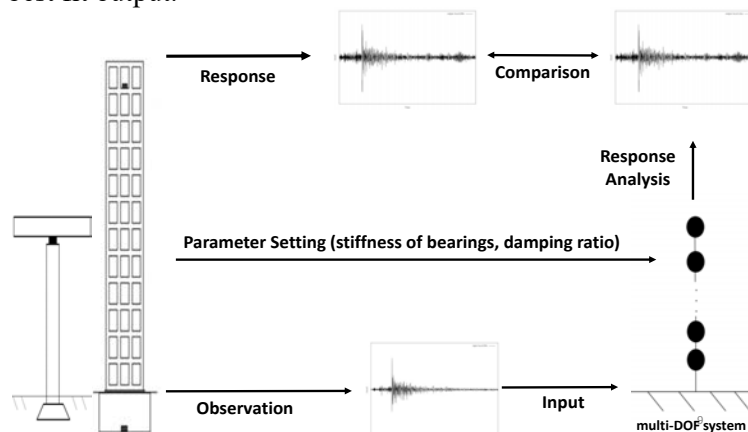


**Fig.8** The outline of the identification method.

The equation of motion for a multi-degree of freedom lumped mass model subjected to earthquake excitation  $\ddot{z}$  can be calculated by the following equations

$$[ \mathbf{M} ]\{\ddot{x}\} + [ \mathbf{C} ]\{\dot{x}\} + [ \mathbf{K} ]\{x\} = -[ \mathbf{M} ]\{\gamma\}\ddot{z} \quad (1)$$

$$x = H(s) \ddot{z} \quad (2)$$

$$H(s) = [-w^2M + iwC + K]^{-1} \quad (3)$$

where  $[ \mathbf{M} ]$ ,  $[ \mathbf{C} ]$  and  $[ \mathbf{K} ]$  stand for mass, damping and stiffness matrices respectively and  $\{ \gamma \}$  stands for the static influence vector. Besides,  $\ddot{x}$ ,  $\dot{x}$  and  $x$  stand for displacement, velocity and acceleration of the lumped mass respectively. By solving the differential equation, the solution of the displacement can be expressed in a form of Eq. (2). where  $H(s)$  stands for the transfer function for this multi-degree of freedom model and can be expressed as the inverse matrix of an independent matrix given as Eq.(3). In this way, the real values of displacement, velocity and acceleration can be calculated by giving the ground earthquake acceleration as an input.

In this case, each block of Matsunohama Viaduct is separated into three parts, which are footing, pier and girder. The target structure was modeled by both 1 DOF model and 2 DOF model. In the case of 1 DOF, the entire superstructure is assumed to move rigidly and the characteristics of the superstructure of Matsunohama Viaduct were identified by using the observation record at the pier top as an input as depicted in Fig.9. In the case of 2 DOF, the entire substructure and the superstructure are assumed to move rigidly and the characteristics of the superstructure of Matsunohama Viaduct were identified by using the observation record at footing as an input. One DOF represents the seismic base isolated superstructure and the other represents the substructure as depicted in Fig.10.

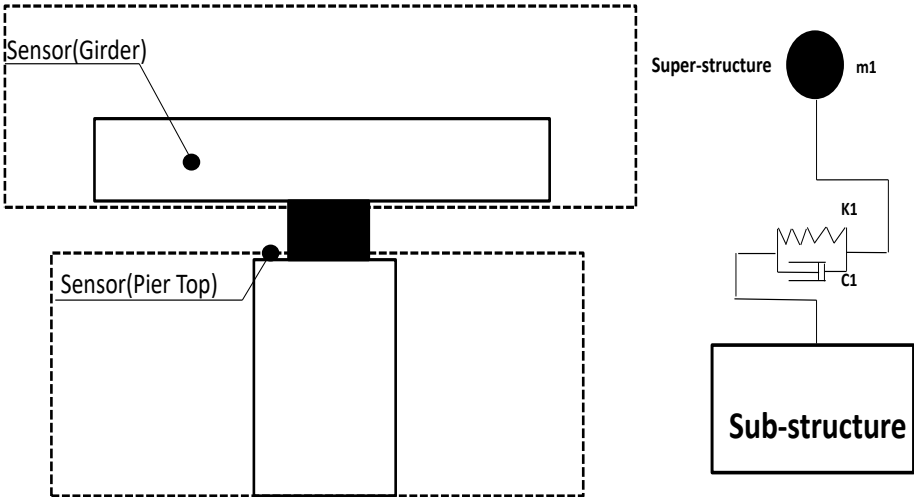
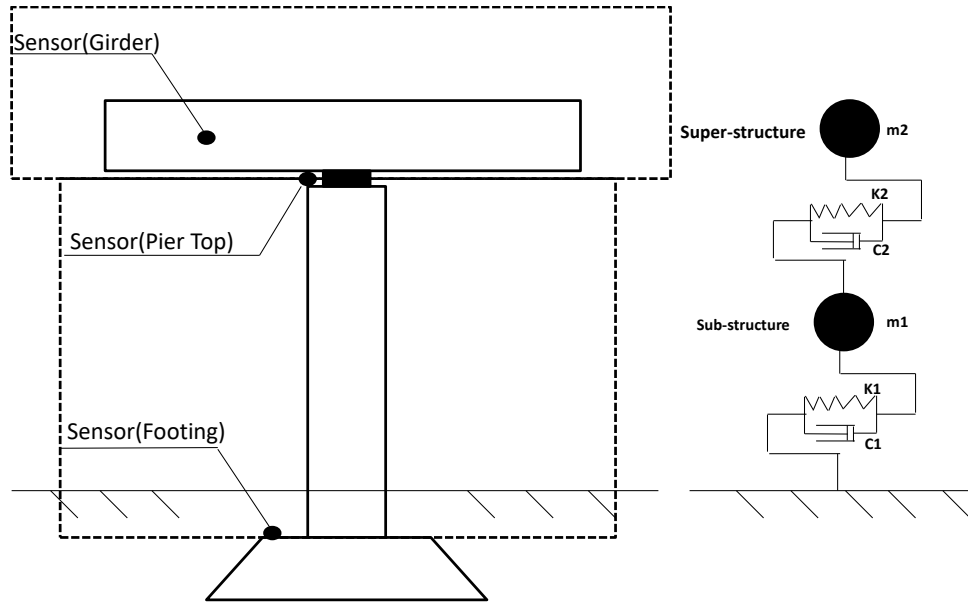


Fig.9 One DOF model of target bridge



**Fig.10** Two DOF model of target bridge

## 5. DISCUSSION ON RD METHOD

In order to estimate the damping ratio of structures, the Random Decrement (RD) technique is applied in this study. RD method is a widely used method to evaluate damping ratio. In the first step, local maximum of the response acceleration were picked up and overlapped one by one to form a RD wave. During this process, the response acceleration  $\dot{x}(t)$  is indicated by the sum of the damped vibration  $\dot{D}(t)$  and the forced vibration  $\dot{R}(t)$ . Since  $\dot{R}(t)$  is a random waveform,  $\sum \dot{R}(t)$  can be offset by overlapping the peaks. On the other hand,  $\sum \dot{D}(t)$  becomes larger and forms a RD wave. So the envelope function of the damped oscillation waveform can be expressed as Eq. (4)

$$\ddot{x}(t) = \{A \sin(\sqrt{1 - h^2} \omega t - \Psi)\} h^2 \omega^2 e^{-h \omega t} \quad (4)$$

where the parameters  $A$ ,  $\omega$ ,  $h$ ,  $\Psi$  stand for the amplitude, frequency, damping ratio and phase difference respectively. This is the principle of the RD method and the damping ratio can be obtained by this method.

The final calculated the damping ratios are summarized as 0.24 for pier and 0.09 for girder in longitude direction. Normally, the damping ratio should be around 2% ~ 8%, with an average of 5%. However, from the table, the calculated results by RD method in this case are much larger than the expected results. Two possibilities are brought up. The first possible reason is that the damping ratio is out the expected range and larger than the expected value in slightly strong earthquake as Takahiro Toyoda et al. [2] once mentioned that the damping ratio was calculated as 0.18 when the shear strain is around 20.8%. Even though the shear strain is slightly larger in comparison with this study, but the value of shear strain is still in the range of small shear strain region conversely. On the other hand, Yusuke et al. [3] claimed that the RD does not fulfill with the assumption in small shear strain region and the possible reasons are listed as follows:

- (1) The RD method is often used in analyzing when the response is stationary, however, we cannot claim that the response is stationary in slightly earthquake situation.
- (2) Since no filter (like Band-pass filter) is used, some noise or other vibration components could be mixed into the RD waveform so that the damping ratio will be overestimated.
- (3) All the local minimum is calculated. Thus some fake peaks or scattered may also be taken into calculation.



Therefore, in this study, the initial setting of damping ratio was set to 5%, the average value according to previous research. For the sake of match, we change the damping ratio manually to find the most satisfied damping ratio during the process of identification.

## 6. TWO-DOF Model SEISMIC RESPONSE ANALYSIS

### 6.1 CASE 1: According to the setting in Design Specification for highway bridges bearings

During the earthquake in Osaka-Fu Hokubu on 18 June 2018, the objective bridge is located in the region, where JMA Seismic Intensity of 4 in the main shock and the corresponding shear strain of the seismic base isolated device is less than 20%. Based on the initial properties of the LRBs installed between the pier top and girder in P408 shown in **Table 2** and designed equation of calculation in “Design Specification for highway bridges bearings”, its shear modulus can be calculated as Eq. (5)

$$K_s = \frac{G(\gamma)A_e}{\sum t_e} \quad (5)$$

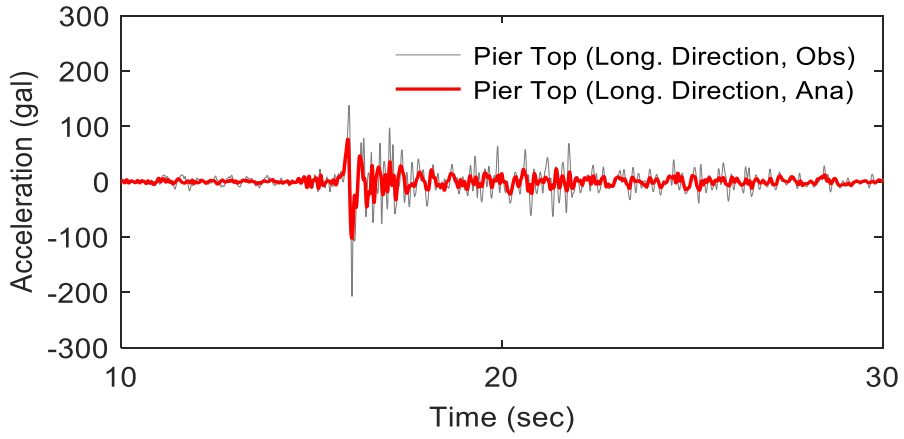
In this case, its primary stiffness  $K_1$  is given as  $59731 \text{ N/mm}$  when the shear strain is less than 80%. Therefore, its corresponding shear modulus remains the constant value of  $9.4 \text{ N/mm}^2$ . Additionally, its damping ratio is increased to 6% manually to match with the recorded data. With this setting, the result of acceleration identification are shown in **Fig.11** and the characteristic properties are summarized in **Table 3**. Based on the best fit result, the maximum displacement in this situation is 1.2 mm and the shear strain is 0.95 in this case. To clarify the frequency response of the vibration, the transfer functions between footing and pier top, footing and girder, pier top and girder are calculated and plotted shown in **Fig.12**. The transfer function between pier top and girder represent the frequency characteristics of the seismic base isolated layer and the peaks for the transfer functions are also summarized in **Table 4**.

**Table 2** Initial setting properties of LRBs

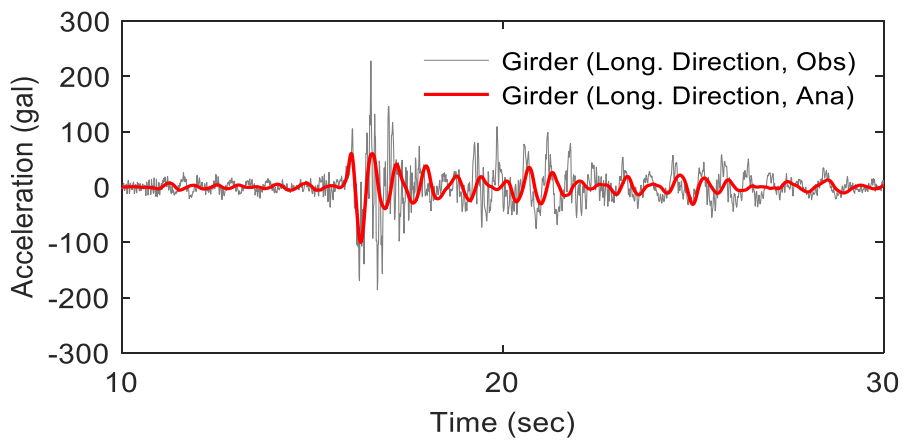
Shear modulus	8	$kg/cm^2$
Width of the bearing	830	mm
Length of the bearing	1030	mm
Diameter of each plug	120	mm
Numbers of the bearings		4
Numbers of rubber layers		6
Thickness of the each rubber layer	21	mm

**Table 3** The characteristic properties (CASE 1)

	MAX[gal]	RMS [gal]
Accl. (Pier Top,obs)	207.2	9.0
Accl. (Pier Top,ana)	89.9	4.8
Accl. (Girder,obs)	227.8	12.8
Accl. (Girder,ana)	97.0	7.3

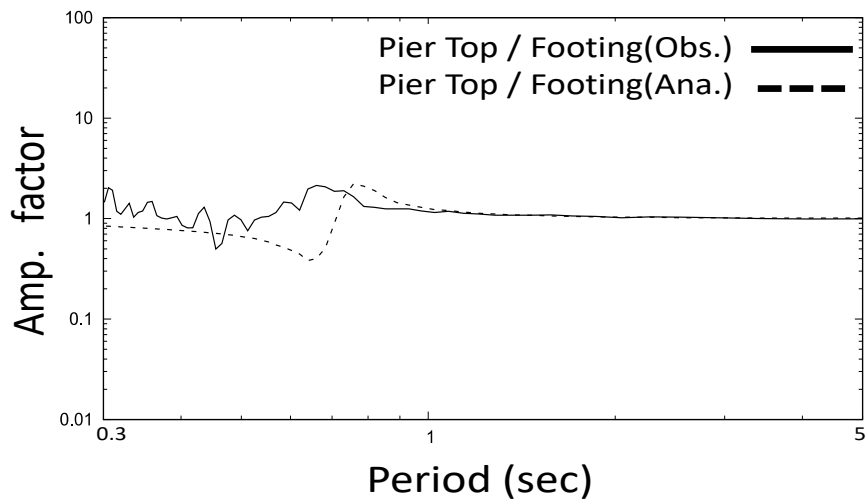


( a ) Acceleration (Pier Top)

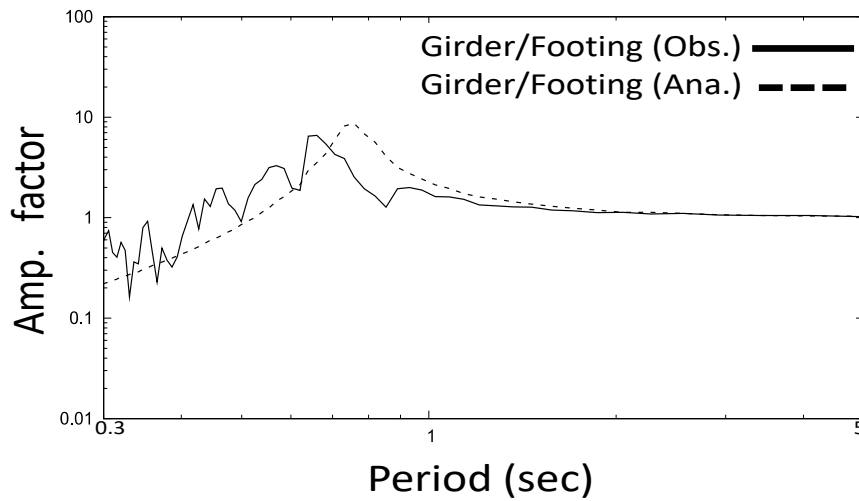


( b ) Acceleration (Girder)

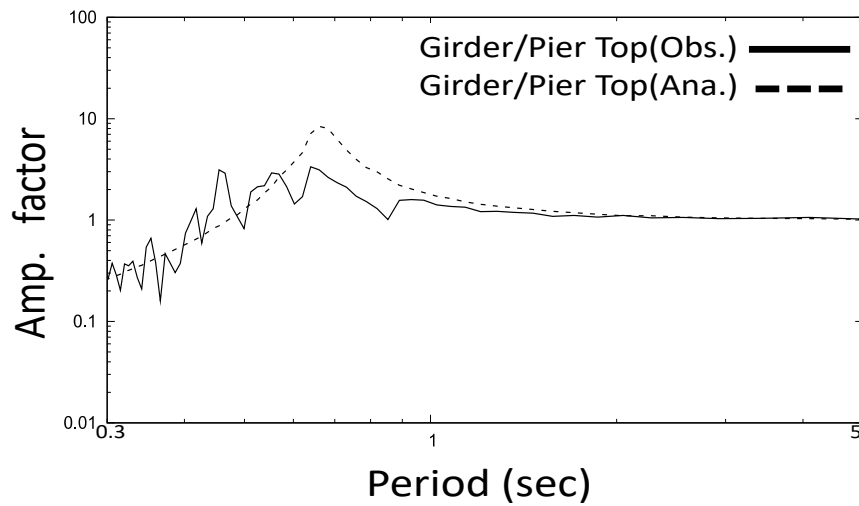
**Fig.11** Identification Result in Long. Direction (CASE 1)



( a ) Pier Top/Footing



( b ) Girder/Footing



( c ) Girder/Pier Top

**Fig.12** Transfer Function in Long. Direction (CASE 1)

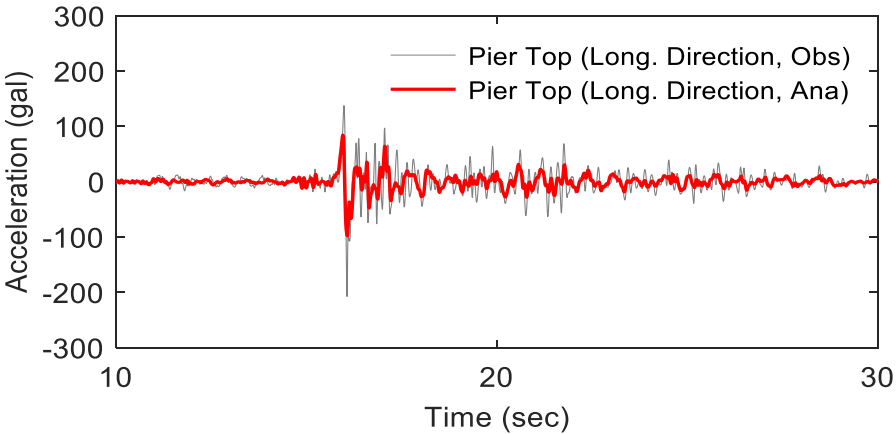
**Table 4** Period when the transfer function reach the peak (CASE 1)

		Period reaches the Peak
Pier Top/Footing	(obs)	0.67
Pier Top/Footing	(ana)	0.78
Girder/Footing	(obs)	0.64
Girder/Footing	(ana)	0.74
Pier Top/Girder	(obs)	0.54(average value)
Pier Top/Girder	(obs)	0.66

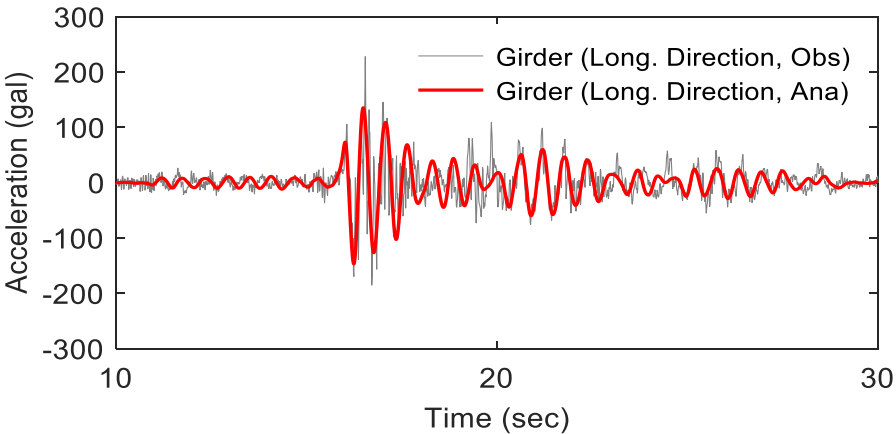
## 6.2 CASE 2: Best fit result

The identification result of identification becomes better with the increasing of the stiffness of the rubber bearings or pier. By this idea, the stiffness of bearings and pier is increased manually to match the observation. The results of acceleration identification are shown in **Fig.13** and the characteristic properties are summarized in **Table 5**. In this situation, its shear modulus was calculated as  $14.7 \text{ N/mm}^2$  for each bearing and the stiffness was set as  $98100 \text{ N/mm}$ . According to the best fit result, the maximum displacement is 1.23 mm and the shear strain is around 0.98%. In this situation, the

transfer functions between footing and pier top, footing and girder, pier top and girder are also been calculated as shown in **Fig.14** to clarify the frequency response of the vibration. The peak for the transfer function is also summarized in **Table 6**. From the comparison, we can find that the identification result of girder does match with the observation records well. However, the difference is still large between the identification result of pier top and recorded data.



( a ) Acceleration (Pier Top)

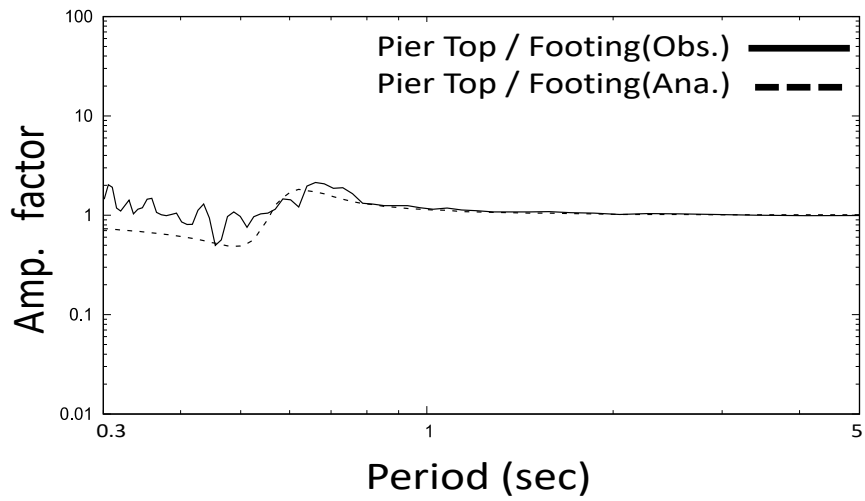


( b ) Acceleration (Girder)

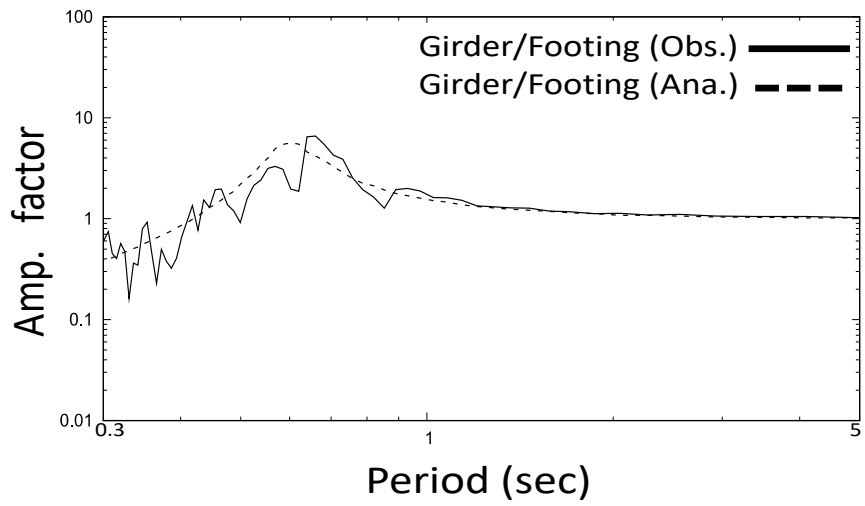
**Fig.13** Identification Result in Long. Direction (CASE 2)

**Table 5** The characteristic properties (CASE 2)

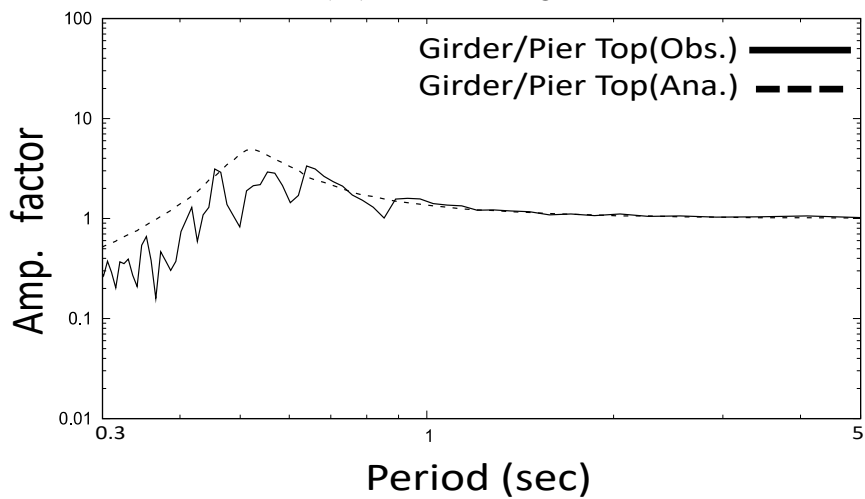
	MAX[gal]	RMS [gal]
Accl. (Pier Top,obs)	207.2	9.0
Accl. (Pier Top,ana)	91.3	5.2
Accl. (Girder,obs)	227.8	12.8
Accl. (Girder,ana)	155.2	11.0



( a ) Pier Top/Footing



( b ) Girder/Footing



( c ) Girder/Pier Top

**Fig.14** Transfer Function in Long. Direction (CASE 2)

**Table 6** Period when the transfer function reach the peak(CASE 2)

		Period reaches the Peak
Pier Top/Footing	(obs)	0.67
Pier Top/Footing	(ana)	0.62
Girder/Footing	(obs)	0.64
Girder/Footing	(ana)	0.60
Pier Top/Girder	(obs)	0.54(average value)
Pier Top/Girder	(obs)	0.53

## 7. ONE-DOF Model Seismic Response Analysis

### 7.1 CASE 1: According to previous research

Junji Yoshida et al.[4] has also done research to evaluate the performance of Matsunohama Viaduct P408 during 1995 Kobe earthquake based on observed records by the model of one degree of freedom system. The corresponding stiffness and damping ratio of the best fit result is given as  $188563 N/mm$  and 13.2% respectively at previous study. We can see that the setting of stiffness is also than the experimental primary stiffness based on this previous research. Two properly reasons caused this discrepancy are the contribution of influence of friction acting on bearings whose magnitude of the friction cannot be ascertained due to uncertainty of the coefficient of friction and the effect of aging, corrosion, humidity, etc. According to this setting, the result of acceleration and velocity identification are shown in **Fig.15** and the characteristic properties are summarized in **Table 7**. The transfer functions between pier top and girder are also been plotted as shown in **Fig.16** whose peak shows at 0.36s. From the comparison of the transfer function, we can see that the previous best fit stiffness setting is larger than the real situation in this case.

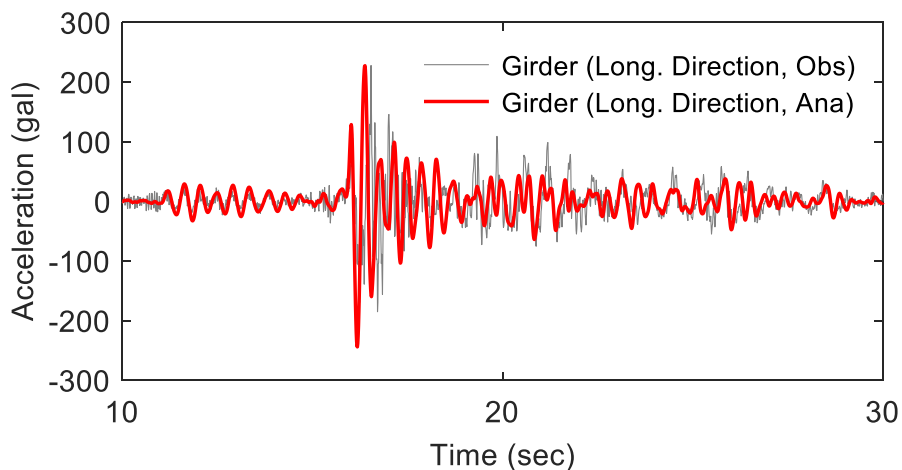


**Fig.15** Identification Result in Long. Direction (Case 1)

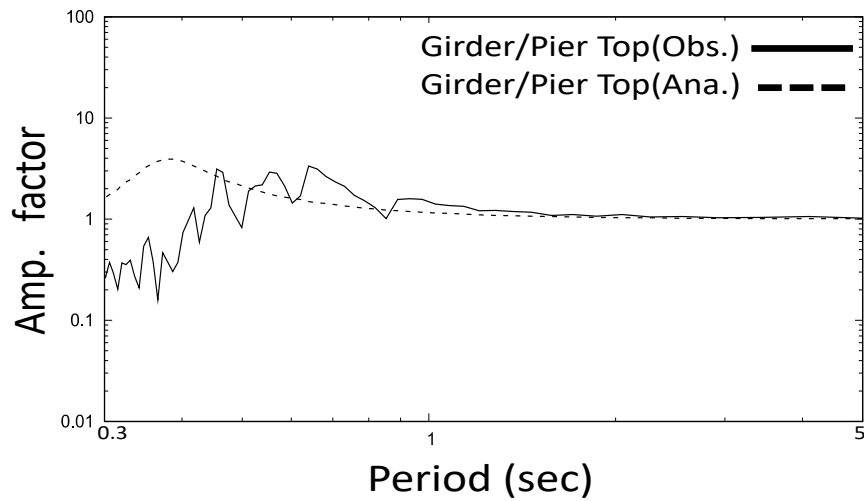


**Fig.16** Transfer Function in Long. Direction (Case 1)

## 7.2 CASE 2: According to previous research

In order to check the relationship between this study and the previous study, we remained the same damping ratio 13.2% and decreased the stiffness to match the observation (Case2-1). The corresponding acceleration identification result is shown in **Fig.17** and the characteristic properties are summarized in **Table 8**. In the second step, the damping ratio is also been slightly decreased to 9% to match with the observation better (Case2-2). The final best fit result of acceleration identification is shown in **Fig.18** and the characteristic properties are summarized in **Table 9**. From the comparison, we can clarify that the actual seismic behavior of the superstructure can be well expressed in this case and both the best fit stiffness and damping ratio is this study is smaller than that in the previous study.

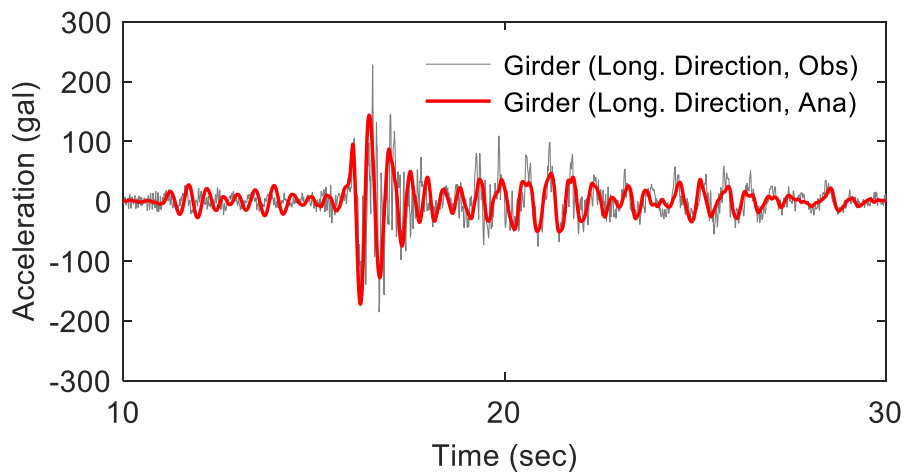


**Fig.17** Identification Result in Long. Direction (CASE 2-1)

**Table 8** The characteristic properties(CASE 2-1)

		MAX[gal]	RMS [gal]
Accl.	(Girder,obs)	227.8	12.8
Accl.	(Girder,ana)	173.3	12.4

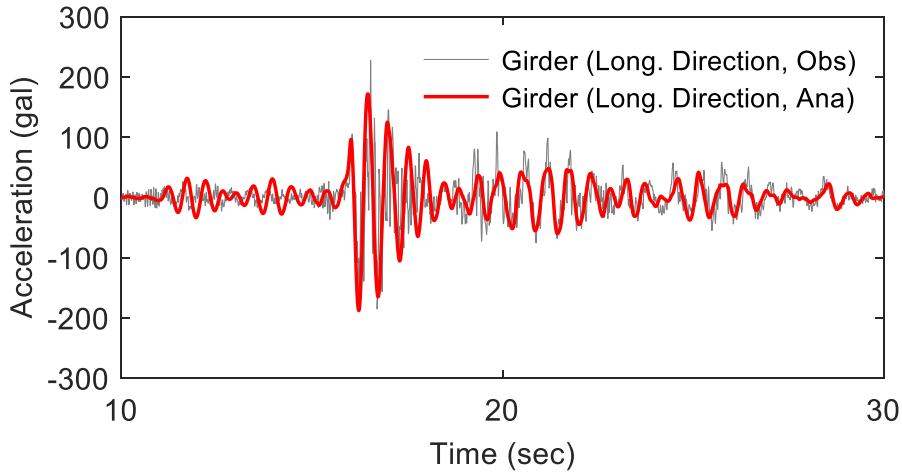


**Fig.18** Identification Result in Long Direction (CASE 2-2)

**Table 8** The characteristic properties (CASE 2-2)

		MAX[gal]	RMS [gal]
Accl.	(Girder,obs)	227.8	12.8
Accl.	(Girder,ana)	187.9	12.7

### 7.3 CASE 3: According to previous research

The acceleration identification result using the setting based on experiment primary stiffness is shown in **Fig.19** and the characteristic properties are summarized in **Table 10**. The transfer functions between pier top and girder among the discussed three situations above have been plotted in **Fig.20**. From the comparison, we can find that the best fit result stiffness obtained in this study as well as in previous research are all larger than the experimental primary stiffness. The influence of friction and the deterioration of the bearings could be two possible reasons. The stiffness should increase over time, however, the best fit stiffness in this study is smaller than that in the previous study. This can state that the influence of friction dominate discrepancy rather than the deterioration of the bearings in the previous study.

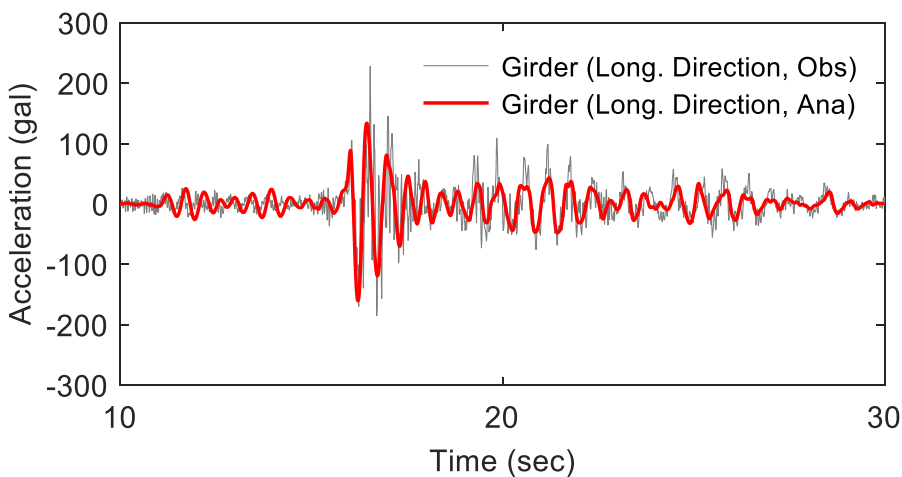


**Fig.19** Identification Result in Long. Direction (Case 3)



**Table 10** The characteristic properties (CASE 3)

		MAX[gal]	RMS [gal]
Accl.	(Girder,obs)	227.8	12.8
Accl.	(Girder,ana)	147.2	12.4

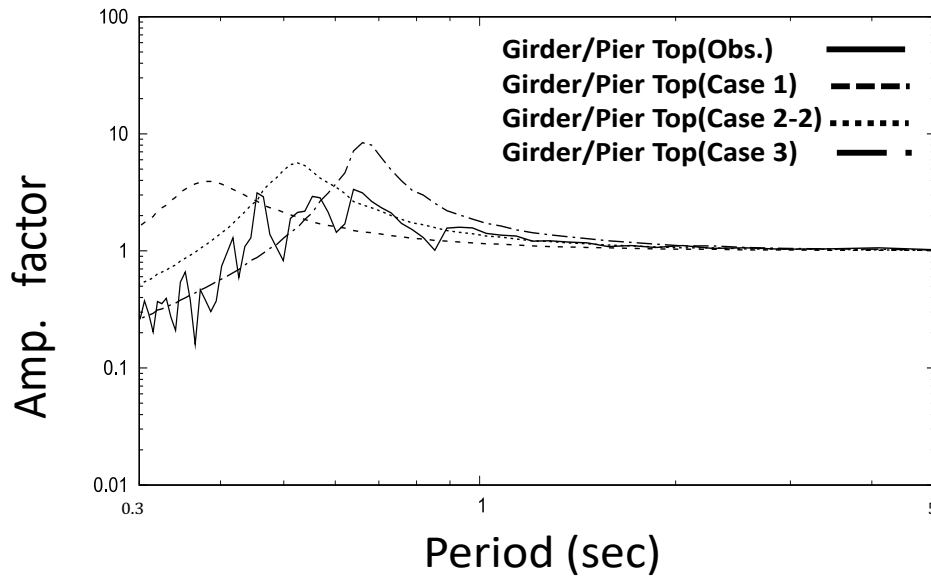


**Fig.20** Transfer Function in Long. Direction

## 8. CONCLUSIONS

It is found that the identified bearing stiffness is larger than the experimental value in slightly strong earthquakes. In this study, the target structure was modeled by both 1 DOF model and 2 DOF model. The actual seismic behavior of the superstructure can be well expressed by 1 DOF model. In the case of 2 DOF, the actual seismic behavior of the superstructure do been well expressed by 2 DOF, however, the difference is still large between the identification result of pier top and recorded data.

## ACKNOWLEDGMENT

The authors would like to thank Hanshin Expressway Corporation and Hanshin Expressway Technology Center for sharing the observation records and information of our target viaducts.

## REFERENCES

- [1] Horimatsu Masayoshi et al. "Vibration Experiments and Dynamic Response Analysis using the actual Highway Bridge with Base Isolators" in Japanese
- [2] Takahiro Toyoda et al. "Estimation the damping ratio of buildings using weak seismic ground motion: A case study on building of the University of Tokyo."
- [3] Yusuke Takeda · Yuuke Kikuchi: Restoring force model of high damping rubber based laminated rubber based on earthquake observation record at small strain, Hokkaido branch of the Japanese Society of Architecture Research Report, pp. 71-74, July 2007 in Japanese
- [4] Junji Yoshida et al. "Performance of base-isolated bridge during 1995 Kobe earthquake based on observed records" from "Proceedings of the Japan Society of Civil Engineers" No-626/ 1-48, 37-50, 1999.7 in Japanese